Water Treatment and Power Co-Generation using Hydrothermal, Supercritical Water Produced by Pulsed Electric Discharges

W. L. Morgan[1] and L. A. Rosocha[2]
[1]Kinema Research and Software, USA
[2]Applied Physics Consulting, LCC, USA

Abstract—Our recent experiments and analyses have demonstrated the possibility of producing supercritical water at high temperatures and densities using a short pulse electric surface discharge in saline solutions. The electrical conductivity of an electrolyte is far greater at the liquid surface than is the bulk conductivity. A short pulse (10 s–100 s ns), high voltage and current surface discharge will then ablate liquid layers, much like laser ablation, driving the ablated fluid to super critical temperatures, pressures and densities above the saturation line, as is found with exploding wires in water. We discuss the experiments, theory, and applications herein.

Keywords—Supercritical water, shock wave, detonation, deflagration, electrolyte, electric discharge, high temperature, high pressure

I. Background

We recently published [1] the results of experiments involving the discharge of a capacitor charged to high voltage across the surface of a salt-water solution. The time scales involved were 10s of nanoseconds to several microseconds. The geometry of the experiment is depicted in Fig. 1. We detected Mach 4 to 8 shock fronts and near sonic bulk fluid flow in the closed test reactor. The 15-20 J of electrical energy deposited was too small to produce such shocks. Similar observations were made by other authors in work published between 1985 and 2001. Their publications are cited in detail in [1].

It is our hypothesis that the short high voltage, high current electrical pulse ablates the salt water surface at pressures above the saturation line, into the supercritical region as shown in Fig. 2. Furthermore, as we discuss below, we propose that the exothermic chemistry occurring in the supercritical electrolyte solution may be sufficient to drive the observed shock waves and fluid behavior as either a detonation or a strong deflagration. Similar $p(T)$ curves occur for exploding wires in water [2].

Fig. 3 shows typical $V(t)$ and $I(t)$ oscilloscope traces from our pulsed discharged experiments in salt water. The flat $V(t)$, $I(t)$, and $P(t)$ for the first ~1.6 μs are evidence of a surface discharge. At that point enough low density vapor, ions, and charged droplets have been transported up between the electrodes that an arc or spark is initiated.

II. Supercritical Water

An important property of water above the critical point, where $p > p_c$ = 220 atm, $T > T_c$ = 374°C, and

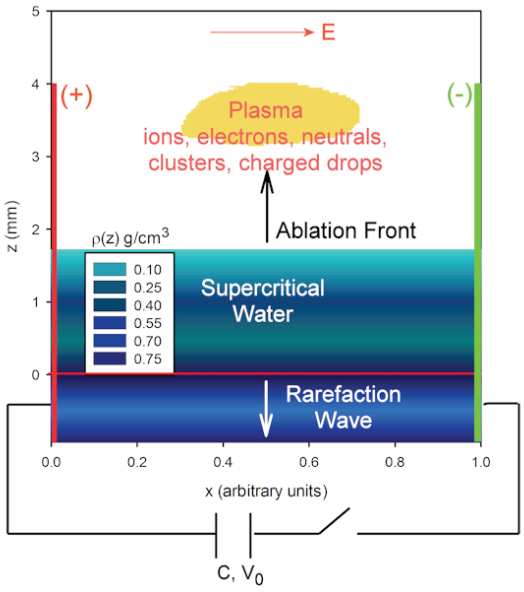

Fig. 1. Geometry of short pulse discharge experiment in salt water.

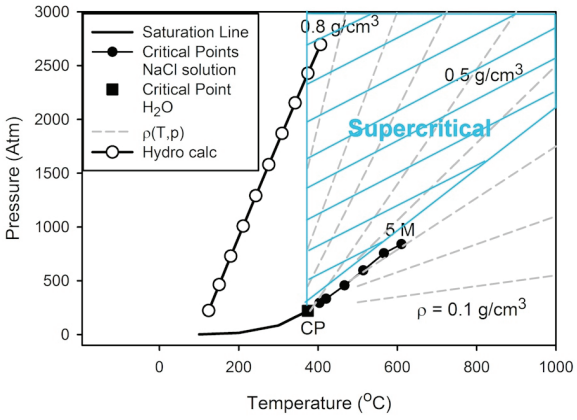

Fig. 2. $p(T)$ from hydrodynamic surface discharge calculation, with no dissipative losses, along with the water saturation line, critical points for 0.5–5 M salt-water solutions, and fluid density $\rho(T, p)$ contours.

Corresponding author: W. Lowell Morgan
e-mail address: morgan@kinema.com

Presented at the 8th International Symposium on Non-Thermal/Thermal Plasma Pollution Control Technology & Sustainable Energy, in June 2012

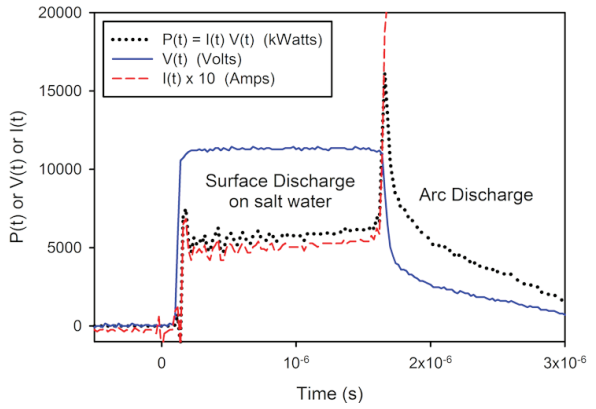

Fig. 3. Short time scale details of pulsed discharge experiment.

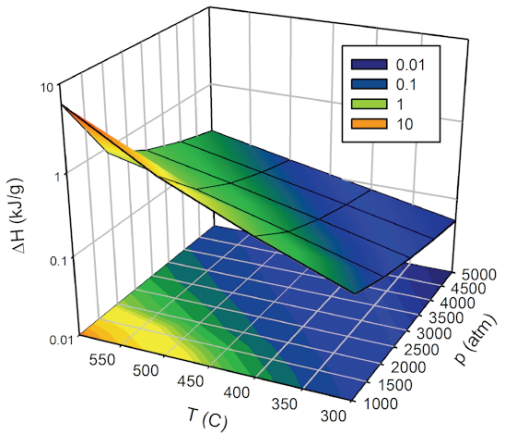

Fig. 4. Exothermicity of ionic chemistry in supercritical 5 M aqueous NaCl solution.

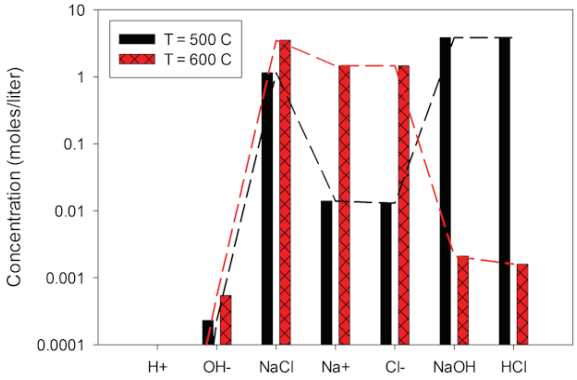

Fig. 5. Equilibrium product concentrations and the amount of water ionized for an initially 5 M NaCl solution comprising only H_2O, Na^+, and Cl^-.

$\rho > 0.35$ g/cm^3, is that the relative dielectric constant ε_r (T, p, ρ) can be much smaller than the $\varepsilon_r \simeq 78$ of liquid water under ordinary conditions. In large regions of the supercritical (T, p, ρ) space ε_r is small enough that the water behaves as a non-polar solvent. Many compounds that are insoluble or immiscible in ordinary water are soluble in supercritical water.

Generally supercritical water is an excellent medium for ionic and free-radical reactions. In ordinary aqueous electrolyte solutions the long range Coulombic interaction of the ions is moderated by the large dielectric constant and the ions become separated by the hydration shells that the polar H_2O molecules form around them. This amounts to reducing the interionic force by a factor of ε_r^{-1}. Consequently, ionic reaction rates are much greater in supercritical water and the equilibrium constants shift toward a mixture of neutral species, such as NaCl, NaOH, or HCl, and away from the near 100% ionic composition found in ordinary water. As all ionic recombination or neutralization reactions are exothermic, heat is released into the system. The rate at which it is released is important.

III. Equilibrium Thermochemistry

There are any number of chemical reactions and species, ionic and neutral, that could be included in a thermochemical model of supercritical salt-water but, following Ho, and Palmer [3] we consider in this study only the following four reactions and eight aqueous species, written as recombination reactions:

$$H^+ + OH^- \Leftrightarrow H_2O \quad (1)$$
$$Na^+ + Cl^- \Leftrightarrow NaCl \quad (2)$$
$$Na^+ + OH^- \Leftrightarrow NaOH \quad (3)$$
$$H^+ + Cl^- \Leftrightarrow HCl \quad (4)$$

subject to the four constraining relations that account for charge and mass conservation.

Each reaction possesses an equilibrium constant K_w^o, K_s^o, K_b^o, and K_a^o using Ho's and Palmer's notation for water, salt, base, and acid respectively. For finite concentrations of the electrolytes the equilibrium constants are modified by the mean activity coefficient $\gamma_\pm$ such that $K_{eq} = K_{eq}^o \gamma_\pm^2$ [4] where $\gamma_\pm$ is a function of the ionic strength, density, dielectric constant of the solvent, and temperature [4, 5]. For very dilute solutions the ionic strength $I \to 1$ and $\gamma_\pm \to 1$.

We obtained the hyperthermal aqueous data using the supercritical properties code SUPCRT92 written by Johnson, Oelkers, and Helgeson [6], which is consistent with the Gibbs' free energy tabulation of Oelkers, *et al.* [7]. Their work covers the temperature range $25^oC \le T \le 1000^oC$ and the pressure range $p_{sat} \le p \le 5000$ bar for values of $\rho \ge 0.35$ g/cm^3.

Fig. 4 shows the exothermicity of the ionic chemistry for a 5 M aqueous NaCl solution for $300^oC \le T \le 600^oC$ and 1000 bar $\le p \le$ 5000 bar, i.e. $\rho \ge 0.35$ g/cm^3. We have not yet extended the Gibbs' free energies of formation, ΔG_f, equilibrium constants K_{eq} (T, p), and enthalpies ΔH_f into the lower density region having $\rho <$ 0.35 g/cm^3.

Fig. 5 shows the final equilibrium concentrations of the eight species at $T = 600^oC$ and $p = 1000$ bars where $\Delta H_r = 6$ kJ/g.

Note that, due to the water being supercritical, the solution has become predominantly neutral. The amount

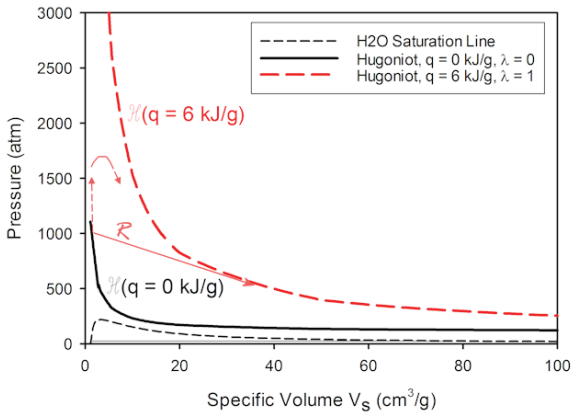

Fig. 6. The Hugoniot curves $\mathscr{H}(\lambda = 0)$ and $\mathscr{H}(\lambda = 1)$ and the Rayleigh "$\mathscr{R}$" line to the Chapman-Jouget (CJ) point.

of heat required to take the solution from 25°C to 600°C is Q = +2 kJ/g and that the heat released by the ionic chemistry in the supercritical solution is 6 kJ/g. This excess exothermicity is what we hypothesize drives a detonation or deflagration front.

In the section we will discuss the time dependence of the chemistry and the physics of detonations and deflagrations.

IV. Detonation and Deflagration Physics

If the aqueous solution is slowly taken from ambient conditions to a supercritical temperature and pressure having a dielectric constant such that the exothermic chemistry can occur, the heat will merely be dissipated in the fluid and flow. In the other limit, if the system is taken to the proper region of (T, p, ρ)–space on a time scale that is short compared to those for heat transfer and hydrodynamic motion, we are proposing that enough exothermic energy may be released to produce a deflagration or detonation front.

If we denote the extent of the reaction sequence by λ, where λ = 0 represents the initial state before reactions have begun and λ = 1 is the limit where the reactions have gone to completion, the hyperbolic Hugoniot curve in (p, v) space, where v is the specific volume $v \equiv 1/\rho$, is written in terms of specific enthalpy h as [8-11]

$$h(p, v, 0 \le \lambda \le 1) - h(p_o, v_o, \lambda = 0) - q(\lambda) + (v + v_o)(p - p_o)/2 = 0$$

The Rayleigh line, which arises from mass flux conservation and is the line of constant detonation velocity D tangent to the Hugoniot, is

$$\rho_o^2 D^2 - (p - p_o)/(v_o - v) = 0$$

where the point of tangency is the Chapman-Jouget point and D is the Mach number.

Fig. 6 graphs the Hugoniot through p = 1000 bar and $v = v$ (600°C, 1000 bar) for λ = 0, the Hugoniot for q (λ = 1) = 6 kJ/g, and the Rayleigh line.

The Rayleigh line shown is that of a deflagration. The dashed curve in Fig. 6 represents a trajectory in p-v space where the exothermicity for $0 < \lambda < 1$ causes an increase in pressure leading to formation of a shock front, which can be a deflagration or detonation depending upon whether $D < 1$ or $D > 1$, respectively.

We have solved the time dependent rate equations for the four water, salt, base, and acid reactions in order to map the dynamic trajectory in (T, p, ρ)-space as a function of time, heat release $q(t) = \Delta h_r(t)$, and $\lambda(t)$. These results are discussed in the next section.

V. Time Dependent Chemistry and Shock Front Dynamics

A. Equation of State

In performing the chemical kinetics calculations with changing values of (T, p, ρ) we need an equation of state (EoS) for the fluid. Accurate but complicated EoS formulations are available for pure water into the supercritical region [12] but not so for salt water above 300°C. We have chosen to use the so-called stiffened gas EoS (SGEoS) [13], which has the form [14, 15]

$$p = C_v(\gamma\text{-}1)T/v - \pi_z$$

where C_v, γ, and π_z are constants. The specific enthalpy h is given by

$$h(T) = C_p T + q_z$$

where C_p and q_z are constants. There are also analytic forms for internal energy, entropy, and Gibbs' free energy. This is essentially a variation on the polytropic gas EoS where the liquid is treated as a very dense gas. We have used the parameters derived by Zein [16], which work moderately well for our purposes.

B. Ionic Reactions

Rates of chemical reactions between positive and negative ions tend to be very large even at liquid densities. In gases at atmospheric pressure the effective bimolecular rate coefficients may exceed 10^{-6} cm^3/s. In dense gases and liquids the rate limiting step in the recombination process is the diffusion of the ions toward one another.

The diffusion limited recombination problem in liquids was first addressed by Debye using the formalism developed by Smoluchowski [17] for colloid statistics. This involved solving what has become known as the Debye-Smoluchowski equation, which amounts to being a drift-diffusion equation [18].

The similarity parameter in this theory is the ratio of the potential and kinetic energies,

$$\phi(r)/kT = e^2/4\pi\varepsilon_o\varepsilon_r rkT \equiv R_c/r$$

for 1-1 electrolytes where R_c is the so-called Onsager radius, i.e. the ionic separation at which the potential and kinetic energies are equal. For an initially uniform random distribution of ionic separations Debye's steady state rate coefficient is

$$k_D = 4\pi R_c D/[\exp(-R_c/R)-1]$$

where R is the ionic reaction radius. The use of the ill-defined R leads to some ambiguity in k_D. For reactions of positive and negative ions $R_c < 0$ and, for supercritical water where ε_r is small, $|R_c| >> R$ leading to [19, 20]

$$k_D \simeq 4\pi R_c D$$

Using Einstein's relation $D = \mu(kT/e)$ where μ is the ion mobility, $k_D \simeq 4\pi e\mu = k_L$; which is Langevin's 1906 expression for the dense gas diffusion limited recombination rate coefficient.

At 25°C the ion diffusion coefficients for H^+, OH^-, Na^+, and Cl^- are 9.31, 5.30, 1.33, and 2.03 in units of 10^{-5} cm^2/s [21]. From classical collision theory $D \propto T^{1/2}/\rho$ [22].

C. ZND Calculations

Given the four ionic reactions involving the eight species, four ionic and four neutral or, at least, contact ions, we have eight first order initial value differential equations for the time dependent species densities. These must then be incorporated into a shock front model.

As is standard practice in calculations such as these, short of using a multidimensional computational fluid dynamics (CFD) code, we have chosen to use the Zel'dovich-von Neumann-Doering (ZND) model [8-11]. This model is based upon the following explicit assumptions:

(1) one dimensional flow,
(2) the shock front is much thinner than the chemical reaction zone so that heat, mass, and radiation transport can be neglected,
(3) the reaction rates are zero ahead of the shock discontinuity and non-zero behind it,
(4) all thermodynamic variables, other than chemical composition, are in local thermodynamic equilibrium (LTE) everywhere.

These approximations are appropriate to the Lagrangian description of fluid flow.

As shown by Zel'dovich and Raizer [8], the neglect of dissipative processes can be relaxed somewhat. Subsequently Abdelazeem and Hoover [23] have demonstrated in a model study of liquid explosives using a Lennard-Jones fluid model and transport coefficients from Enskog theory that the ZND approximation works quite well on such problems. Fickett and Davis [10] and Law [11] provide the sets of ZND relations that can be applied directly to the model. Using these equations and given the initial (T, p, ρ), [H_2O], [Na^+] = [Cl^-], rate coefficients, and equilibrium constants, we can model the deflagration or detonation propagation.

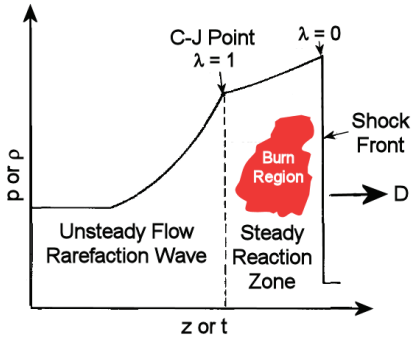

Fig. 7. Depiction of regions of a shock wave in laboratory coordinates.

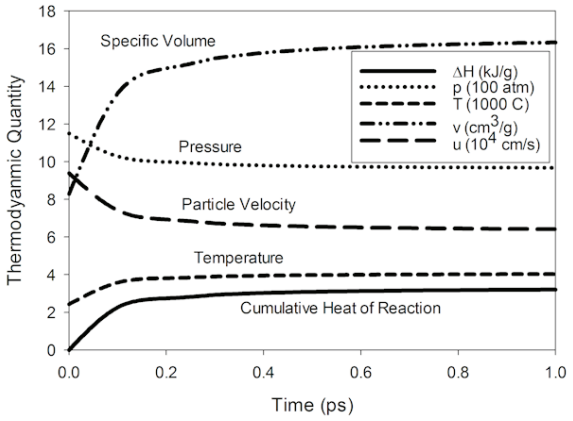

Fig. 8. Time evolution of various thermodynamic properties behind the shock discontinuity in the ZND model. The ambient conditions ahead of the shock front are $T = 600°C$, $p = 1000$ atm, and $u = 0$.

The model calculation presented here is for $T_o = 600°C$ and $p_o = 1000$ bar. We have taken $q_{max} = 6$ kJ/g and define $\lambda(t)$, the extent of reaction, as

$$\lambda(t) \equiv \int[(dq(t)/dt]dt/q_{max}$$

where $0 \le \lambda(t) \le 1$. Although $\lambda = 1$ corresponds to an energy release of q_{max} in the equilibrium calculation, i.e. $q(t\to\infty) = q_{max} \Rightarrow \lambda(t\to\infty) = 1$, the short non-equilibrium time scale $\lambda(t)$ generally does not reach unity until far behind the leading edge of the shock front. As the kinetics change with (T, p, ρ) behind the shock front, λ may not reach unity at all.

D. Computational Results using ZND Theory

Fig. 7 is a schematic of the shock front propagation showing the important physical regions and quantities. In the ZND model the shock front itself is a propagating discontinuity whereas, if dissipation processes are included [8, 23], its thickness becomes finite.

Fig. 8 graphs the temperature $T(t)$, pressure $p(t)$, specific volume $v(t)$, particle velocity $u(t)$, and extent of reaction $\lambda(t)$ behind the shock front. The sound speed in

the supercritical water, $C_s = (\gamma p_o/\rho_o)^{1/2}$, is 5.9×10^4 cm/s and the shock speed is Mach 2.

The rate coefficients for the ionic recombination range over $10^{-9} \le k_D \le 4\times10^{-8}$ cm^3/s. These are several orders of magnitude smaller than they would be in the gas phase at atmospheric pressure but several powers of ten larger than neutral reaction rates in fluids. Due to the large rate coefficients the chemistry time scale is picoseconds, as shown in Fig. 8.

We have, herein, used only the simplest expressions for the ionic diffusion and recombination coefficients. The dependencies of the coefficients upon ion concentrations, inter-ionic density distribution, and time have been ignored. These, indeed, remain topics of contemporary research in physical chemistry.

Typically in a Mach > 1 detonation in a gas the leading edge of the shock compresses and heats the gas, as depicted in Fig. 7, and the exothermic chemistry occurs for some distance behind the shock. In the model for our experiment the short pulse surface discharge drives the ablating water to high temperature and pressure, which is indicated in Figs. 1 and 2. As shown in Fig. 4 there may be a region in (T, p, ρ) in the supercritical salt water where the ionic chemistry has enough exothermicity to produce a detonation or deflagration front. The shock propagates outward into the less dense region where, due to the rapidity of the ionic reactions, the reaction zone behind the shock is very thin. This is similar thermodynamically to the Diesel cycle. At some point, 1-3 μs into the experiment, as seen in Fig. 3, the fluid comprising neutral and ionic species is rarified enough that the applied voltage can break it down and ignites the arc. We have not performed any modeling of the arc.

There is a great amount of uncertainty in the energetics of the overall process and of the sub-processes due in part to a dearth of thermochemical data for electrolyte solutions in the region of supercritical (T, p, ρ)-space under discussion here. In addition, our cobbled together 1-d hydrodynamic calculation and ZND shock model, which lack dissipative processes, leave much to be desired. A good hydrodynamic code having a dimensionality of one or greater should be able to address the computational aspects of this problem reasonably well. In our experiments [1] we were not able to field diagnostics of sufficient sophistication to provide truly high quality data. Good data in this regime between the supercritical state and a full fledged plasma state are difficult, at best, to obtain.

VI. Potential Applications

Although our experiments [1] consisted of a single pulse microsecond time scale discharge on a thin film of salt water, it could in principle be pulsed with a repetition rate of, say, 1 kHz. As it is very simple, a large number of such reactors could be replicated in parallel, hence processing a significant volumetric flow rate while simultaneously recovering some of the power expended. Processing of industrial waste via supercritical water oxidation (SCWO) and subsequent power co-generation has been a topic of research for a long time. This is the first proposal that we know of to produce and utilize SCWO in a short pulse process.

A. Urea Chemistry

Urea, $(NH_2)_2CO$, is a very common organic molecule, in part because it is a prominent constituent of urine. Urea has the same chemical formula as ammonium cyanate, $[NH_4^+][NCO^-]$, but a different structure. One is transformed into the other with NH_3 and HNCO as intermediate species.

At 25^{o}C urea decomposes in aqueous solution at the rate of 7×10^{-5} moles/liter/day. Above 65^{o}C the urea isomeric decomposition rate increases dramatically. In acidic solutions the ammonium cyanate is rapidly converted to NH_3 and CO_2.

Urine is ~95% water and comprises about 9.3 g/L urea, 1.9 g/L chloride, 1.2 g/L sodium, 0.8 g/L chloride, 1.2 g/L sodium, 0.8 g/L potassium and small concentrations of other ions, in organic, and organic substances. Thus urine is about a 0.03 molar saline solution and a 0.16 molar aqueous urea solution.

That aqueous urea ultimately forms NH_3 and CO_2 under acidic conditions implies that a supercritical solution may have properties different from those of a solution under ordinary conditions. There have been a number of studies in recent years of hydrothermal, supercritical urea solutions.

The urea decomposition process in supercritical water is

$$(NH_2)_2CO \rightarrow NH_4^+ + OCN^-$$

followed by

$$NH_4^+ + OCN^- + H_2O \rightarrow CO_2 + 2NH_3$$

Okazaki and Funazukuri [24] have observed that, for temperatures $T > T_c$, the addition of NaCl enhanced the rate coefficient for urea composition and that the addition NaOH produced a great enhancement of the rate. The overall process is exothermic. Another possible reaction channel may produce H_2.

B. Wastewater Treatment

A typical wastewater chemical analysis might show the following concentrations of contaminants in mg/L:

Biochemical oxygen demand (BOD)	220
Total organic carbon (TOC)	160
Chemical oxygen demand (COD)	500
Total Nitrogen (as N)	40
Total phosphorous (as P)	8
Chlorides	50
Sulfates	30

Alkalinity (as $CaCO_3$)	100

where ~1/3 of the N is organic and ~2/3 is free ammonia. ~1/3 of the P is organic and ~2/3 is inorganic. An increasing, but small, fraction of the TOC comprises remnants of medications ranging from vitamins to psycho-pharmaceuticals such as bupropion-hydrochloride ($C_{13}H_{18}ClNO{\bullet}HCl$), which is well known under its brand name Wellbutrin.

As population increases, the planet warms, and clean fresh water becomes relatively more scarce, treatment of wastewater becomes a topic of increasing importance. Standards for removal of nitrogen and phosphorous from wastewater are becoming more strict because of their contributions as nutrients to the biological pollution of streams, lakes, and even the Gulf of Mexico.

Many researchers are investigating the use of hydrothermal supercritical water oxidation (SCWO) for treatment of wastewater and biomass. Because of the generally large exothermicity of the chemistry under supercritical conditions, SCWO is of great interest due to its potential for power co-generation [25]. What we have presented here may be a scalable approach to SCWO treatment of water.

REFERENCES

[1] W. L. Morgan and L. A. Rosocha, "Surface electrical discharges and plasma formation on electrolyte solutions," *Chemical Physics*, vol. 398, pp. 255-261, 2012.

[2] A. Grinenko, V. T. Gurovich, Y. E. Krasik, and Y. Dolinsky, "Addressing water vaporization in the vicinity of an exploding wire," *Journal of Applied Physics*, vol. 100, 113309, 2006.

[3] P. C. Ho, and D. A. Palmer, "Electrical conductivity measurements of aqueous electrolyte solutions at high temperatures and pressures," unpublished.

[4] J. Chlistunoff, K. J. Ziegler, L. Lasdon, and K. P. Johnson, "Nitric/nitrous acid equilibria in supercritical water," *Journal of Physical Chemistry A*, vol. 103, pp. 1678-1688, 1999.

[5] M. R. Wright, *An Introduction to Aqueous Electrolyte Solutions*, Chichester, England: Wiley, 2007.

[6] J. W. Johnson, E. H. Oelkers, and H. C. Helgeson, "SUPCRT92: A software package for calculating the standard molal thermodynamic properties of minerals, gases, aqueous species, and reactions from 1 to 5000 bar and 0 to 1000ºC," *Computers and Geosciences*, vol. 18, pp. 899-947, 1992.

[7] E. H. Oelkers, H. C. Helgeson, E. L. Shock, D. A. Sverjensky, J. W. Johnson, and V. A. Pokrovskii, "Summary of the Apparent Standard Partial Molal Gibbs Free Energies of Formation of Aqueous Species, Minerals, and Gases at Pressures 1 to 5000 Bars and Temperatures 25 to 1000ºC," *Journal of Physical and Chemical Reference Data*, vol. 24, pp. 1401-1560, 1995.

[8] Ya. B. Zel'dovich and Yu. P. Raizer, *Physics of Shock Waves and High-Temperature Hydrodynamic Phenomena*, Mineola, NY: Dover, 2002.

[9] L. D. Landau and E. M. Lifshitz, *Fluid Mechanics*, Singapore: Elsevier, 2004.

[10] W. Fickett and W. C. Davis, *Detonation Theory and Experiment*, Mineola, NY: Dover, 1979.

[11] C. K. Law, *Combustion Physics*, New York, NY: Cambridge University Press, 2006.

[12] C. A. Jeffery and P. H. Austin, "A new analytic equation of state for liquid water," *Journal of Chemical Physics*, vol. 110, pp. 484-496, 1999.

[13] R. Menikoff and B. J. Plohr, "The Riemann problem for fluid flow of real materials," *Reviews of Modern Physics*, vol. 61, pp. 75-130, 1989.

[14] F. Petitpas, J. Massoni, R. Saurel, E. Lapebie, and L. Munier, "Diffuse interface model for high speed cavitating underwater systems," *International Journal of Multiphase Flow*, vol. 35, pp. 747-759, 2009.

[15] A. Zein, M. Hantke, and G. Warnecke, "Modeling phase transition for compressible two-phase flows applied to metastable liquids," *Journal of Computational Physics*, vol. 229, pp. 2964-2998, 2010.

[16] A. Zein, "On the numerical simulation of a laser-induced cavitation bubble with phase transition," unpublished.

[17] S. Chandrasekhar, "Stochastic problems in physics and astronomy," *Reviews of Modern Physics*, vol. 15, pp. 1-89, 1943.

[18] M. R. Flannery, "Theory of Ion--Ion Recombination," *Philosophical Transactions of the Royal Society of London. Series A, Mathematical and Physical Sciences*, vol. 304, pp. 447-497, 1982.

[19] S. A. Rice, P. R. Butler, M. J. Pilling, and J. K. Baird, "A solution of the Debye-Smoluchowski equation for the rate of reaction of ions in dilute solution," *Journal of Chemical Physics*, vol. 70, pp. 4001-4007, 1979.

[20] K. Wolf and W. M. Bartczak, "Dynamics of diffusion-controlled recombination of ions in ionic solutions. Limits of validity of the Debye - Smoluchowski equation," in *Proceedings of SPIE - The International Society for Optical Engineering*, 2000, pp. 137-148.

[21] D. G. Leaist and B. Wiens, "Interdiffusion of acids and bases. HCl and NaOH in aqueous solution," *Canadian Journal of Chemistry*, vol. 64, pp. 1007-1011, 1986.

[22] J. O. Hirschfelder, C. F. Curtiss, and R. B. Bird, *Molecular Theory of Gases and Liquids*, New York: Wiley, 1954.

[23] M. S. Abdelazeem and W. G. Hoover, "One-dimensional dense-fluid detonation wave structure," *Journal of Physical Chemistry*, vol. 87, pp. 2795-2798, 1983.

[24] M. Okazaki and T. Funazukuri, "Decomposition of urea in sub- and supercritical water with/without additives," *Journal of Materials Science*, vol. 43, pp. 2316-2322, 2008.

[25] F. Jimenez-Espadafor, J. R. Portela, V. Vadillo, J. Sanchez-Oneto, J. A. B. Villanueva, M. T. Garcia, and E. J. M. de la Ossa, "Supercritical Water Oxidation of Oily Wastes at Pilot Plant: Simulation for Energy Recovery," *Industrial & Engineering Chemistry Research*, vol. 50, pp. 775-784, 2011.